Development 133, 33-42 doi:10.1242/dev.02172

# Increasing *Fgf4* expression in the mouse limb bud causes polysyndactyly and rescues the skeletal defects that result from loss of *Fgf8* function

**Pengfei Lu[1], George Minowada[1,2,*] and Gail R. Martin[1,†]**

A major function of the limb bud apical ectodermal ridge (AER) is to produce fibroblast growth factors (FGFs) that signal to the underlying mesenchyme. Previous studies have suggested that of the four FGF genes specifically expressed in the mouse AER, *Fgf8* is unique not only in its expression pattern, but also because it is the only such FGF gene that causes limb skeletal abnormalities when individually inactivated. However, when both *Fgf8* and *Fgf4* are simultaneously inactivated in the AER, the limb does not develop. One possible explanation for these observations is that although both of these FGF family members contribute to limb development, *Fgf8* has functions that *Fgf4* cannot perform. To test this hypothesis, we used a novel method to substitute *Fgf4* for *Fgf8* expression in the developing limb bud by concomitantly activating a conditional *Fgf4* gain-of-function allele and inactivating an *Fgf8* loss-of-function allele in the same cells via Cre-mediated recombination. Our data show that when *Fgf4* is expressed in place of *Fgf8*, all of the skeletal defects caused by inactivation of *Fgf8* are rescued, conclusively demonstrating that FGF4 can functionally replace FGF8 in limb skeletal development. We also show that the increase in FGF signaling that occurs when the *Fgf4* gain-of-function allele is activated in a wild-type limb bud causes formation of a supernumerary posterior digit (postaxial polydactyly), as well as cutaneous syndactyly between all the digits. These data underscore the importance of controlling the level of FGF gene expression for normal limb development.

**KEY WORDS: Cutaneous syndactyly, FGF signaling, Limb development, Apical ectodermal ridge, SHH/FGF loop, Interdigital programmed cell death, Polydactyly, Mouse**

## INTRODUCTION

The apical ectodermal ridge (AER), a specialized epithelium that rims the distal tip of the limb bud, is a major source of signals required for vertebrate limb development (Martin, 1998; Capdevila and Izpisua Belmonte, 2001). In the mouse, AER formation begins at the stage when the limb bud can first be discerned. It involves the initiation of gene expression that later marks the mature AER, movement distally of cells within the epithelium (particularly on the ventral side of the limb bud) and changes in cell shape. After the AER matures into a narrow band of pseudostratified columnar cells, it persists for 3-4 days while the limb bud enlarges and cells in the underlying mesenchyme become determined to form the progenitors of the skeletal elements and some of the other mesodermal cell types in the mature limb. At the end of this period, cells in the AER die and the AER regresses (Guo et al., 2003).

The importance of the AER has been well-established by experiments in the chicken embryo showing that AER removal causes limb truncations (Saunders, 1948; Summerbell, 1974; Rowe and Fallon, 1982), and that this is due primarily to death of the underlying limb bud mesenchyme (Rowe et al., 1982; Dudley et al., 2002). The fact that such limb truncations can be rescued by implanting beads soaked in FGF proteins (Niswander et al., 1993; Fallon et al., 1994) indicates that an important function of the AER is to produce FGFs. In addition to sustaining cell survival in limb bud mesenchyme (Sun et al., 2002; Boulet et al., 2004), FGF signaling from the AER is thought to be an essential component of a positive gene regulatory feedback loop that maintains the expression of sonic hedgehog (*Shh*) and its downstream targets in the mesenchyme (Laufer et al., 1994; Niswander et al., 1994), and also to regulate the expression of other genes vital for limb development (Martin, 1998; Capdevila and Izpisua Belmonte, 2001).

Of the 22 mouse genes that encode FGF ligands (Itoh and Ornitz, 2004), four (*Fgf4*, *Fgf8*, *Fgf9* and *Fgf17*) are expressed in the AER but not in other cells in the limb bud. *Fgf8* is unique among these 'AER-FGFs' in several respects. *Fgf8* expression is first detected in AER progenitors in the ventral ectoderm, and subsequently along the entire anteroposterior (AP) length of the AER until it regresses (Crossley and Martin, 1995; Mahmood et al., 1995). By contrast, *Fgf4*, *Fgf9* and *Fgf17* expression commences only after the AER has fully formed, is restricted to the posterior half to two-thirds of the AER, and ceases at least 1 day before AER regression (Sun et al., 2000). Furthermore, gene knockout studies have shown that when each of the AER-FGFs is individually inactivated, only loss of *Fgf8* function causes limb abnormalities (Lewandoski et al., 2000; Moon and Capecchi, 2000); no defects have been detected in *Fgf4* (Moon et al., 2000; Sun et al., 2000), *Fgf9* (Colvin et al., 2001) or *Fgf17* (Xu et al., 2000) null limbs. However, *Fgf4* is essential in the absence of *Fgf8*, because if both *Fgf4* and *Fgf8* are never expressed in the limb bud, the limb does not form (Sun et al., 2002; Boulet et al., 2004).

One model to explain these observations is based on the premises that a certain amount of AER-FGF is required at each stage of limb development, and that the contributions made by FGF4 and FGF8 (and perhaps the other AER-FGFs) to the ligand pool are functionally similar. According to this model, there are two reasons

[1]Department of Anatomy and Program in Developmental Biology, School of Medicine, University of California at San Francisco San Francisco, CA 94143-2711, USA. [2]Department of Medicine, Division of Pulmonary and Critical Care Medicine, Case Western Reserve University, School of Medicine, University Hospitals of Cleveland, Cleveland, OH 44106, USA.

*Present address: Kaiser Permanente, Vallejo, CA 94589, USA
†Author for correspondence (e-mail: gmartin@itsa.ucsf.edu)

**Accepted 27 October 2005**

why inactivation of *Fgf8*, but not of other individual AER-FGF genes, causes abnormalities in limb development. First, at some stages (e.g. in the early and late limb bud) *Fgf8* is the only AER-FGF gene that is expressed and thus is contributing to the ligand pool. Second, at stages when all four AER-FGF genes are co-expressed in the posterior limb bud, *Fgf8* is expressed more abundantly and more broadly than the others, and therefore makes a more substantial contribution to the ligand pool. In either case, when any other AER-FGF gene is individually is inactivated, the total amount of ligand in the pool does not fall below the level needed for normal limb development. However, when both *Fgf4* and *Fgf8* are completely inactivated, there is insufficient ligand to sustain limb development. An alternative model is that FGF8 has unique functions in limb skeletal patterning that FGF4 (and presumably the other AER-FGFs) cannot perform.

To distinguish between these models and to determine the consequences of increasing *Fgf4* expression in the limb bud, we employed a conditional gain-of-function (GOF) approach. We found that activating an *Fgf4*$^{GOF}$ transgene in wild-type limb buds, in a domain that largely resembles that of *Fgf8* in the normal limb bud, caused several abnormalities, including formation of a supernumerary posterior digit (postaxial polydactyly) and inhibition of programmed cell death in the interdigital mesenchyme, resulting in retention of tissue between the digits (cutaneous syndactyly); together these phenotypes are termed polysyndactyly. Activation of the *Fgf4*$^{GOF}$ transgene in an *Fgf8*-null limb bud still caused polysyndactyly, but it also rescued all the skeletal defects that result from loss of *Fgf8* function. Together, these data support the hypothesis that AER-FGF signaling plays a role in regulating digit number and cell death in the interdigital mesenchyme, and that FGF4 and FGF8 perform similar functions in patterning the limb skeleton.

## MATERIALS AND METHODS

### Production of a mouse line carrying an *Fgf4*$^{GOF}$ transgene

To construct the *Fgf4*$^{GOF}$ transgene, we replaced the human placental alkaline phosphatase sequence in the Z/AP vector (Lobe et al., 1999) (kindly provided by Dr Andras Nagy) with a fragment of a mouse cDNA containing the entire *Fgf4* open reading frame. The *Fgf4* and *loxP* segments of the resulting construct (Fig. 1A) were sequenced to confirm that no mutations had arisen during vector construction.

The construct was electroporated into a subclone of E14Tg2a ES cells (Hooper et al., 1987) isolated by A. Smith (kindly provided to us by W. Skarnes). A total of 384 G418-resistant clones were isolated, and an aliquot

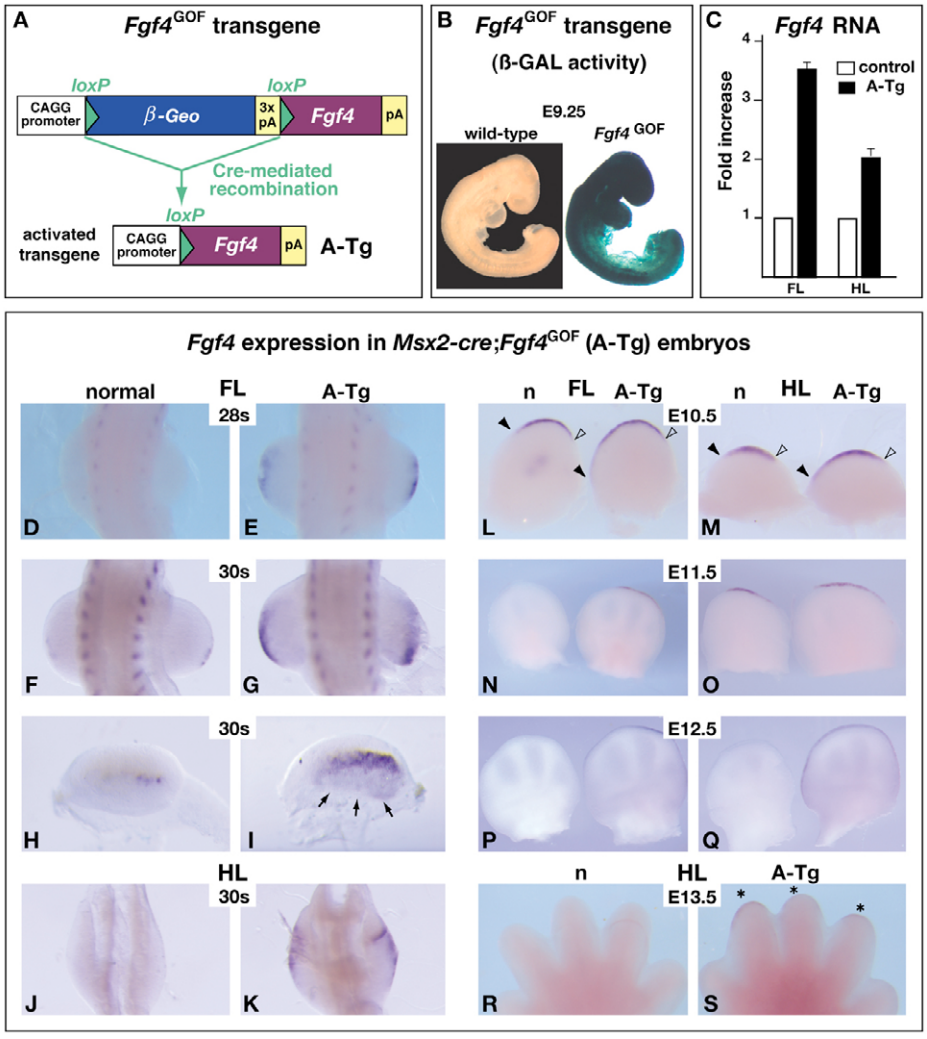


**Fig. 1. *Fgf4* expression in limb buds following Cre-mediated activation of a conditional *Fgf4* gain-of-function allele.** (**A**) Schematic representation of the *Fgf4*$^{GOF}$ transgene, in which the CAGG promoter drives expression of the β-Geo gene, and the triple polyadenylation sequence (3× pA) prevents expression of sequences downstream of the β-*Geo* gene. Cre-mediated recombination deletes the β-Geo gene and the 3× pA, and as a result, the previously silent downstream mouse *Fgf4* cDNA is expressed from the 'activated' transgene (A-Tg). (**B**) An assay for *lacZ* expression [β-galactosidase (β-gal) activity] in whole mount shows that the CAGG promoter drives expression of the *Fgf4*$^{GOF}$ transgene in a wide variety of cell types at E9.5. The *Fgf4*$^{GOF}$ embryo shown is hemizygous for the transgene. (**C-S**) *Fgf4* expression is compared in limb buds from normal (n) and *Msx2-cre*;*Fgf4*$^{GOF}$ embryos, in which the transgene has been activated (A-Tg). (C) Relative levels of *Fgf4* expression as assessed by quantitative RT-PCR (see Materials and methods). (D-S) *Fgf4* expression as detected by whole-mount RNA in situ hybridization at the stages indicated. In the *Msx2-cre*;*Fgf4*$^{GOF}$ limb buds, the in situ hybridization signal represents the sum of *Fgf4* RNA produced by the endogenous *Fgf4* locus and the activated transgene. All panels show dorsal views, except H,I, which show distal views of the limb buds with dorsal at the top. In D-G,J,K anterior is towards the top; in all other panels, anterior is towards the left. The arrows in I indicate the domain of *Fgf4* expression in the ventral ectoderm. The filled and open arrowheads in L,M indicate the anterior and posterior ends, respectively, of the *Fgf4* expression domain in the AER. At E13.5, *Fgf4* expression in the *Msx2-cre*;*Fgf4*$^{GOF}$ limb bud is restricted to the AER covering the distal tips of the digit primordia (asterisks). Abbreviations: FL, forelimbs; HL, hindlimbs; s, somite stage.

of each clone was assayed for β-galactosidase (β-gal) activity (Lobe et al., 1999). Of these, the 36 clones with the strongest and most uniform staining were selected for further study. An aliquot of each was frozen, and another aliquot was expanded and cultured under conditions appropriate for embryoid body formation (Martin and Evans, 1975). To obtain differentiation to a wide variety of cell types, the embryoid bodies from each clone were allowed to attach to a tissue culture surface. After ~8-10 days of culture, when differentiated cells including rhythmically contracting myocardial cells were observed, the cells were fixed and stained for β-gal activity. Nine of the clones were chosen for further analysis because their differentiated derivatives almost all displayed strong β-gal activity; in the remaining clones, β-gal activity was either weak or not detected in their differentiated derivatives. Chromosome analysis was performed on six out of these nine clones, and more than 80% of the cells examined for each clone were found to contain 40 chromosomes. When assayed by Southern blotting using a variety of restriction enzymes, the transgene in all of these six clones appeared to have inserted into a single site.

Two of these ES cell clones were injected into C57BL/6 blastocysts by the Stanford University transgenic facility, and germ-line transmission of the *Fgf4*$^{GOF}$ transgene was obtained from male chimeras produced from one of these cell lines. The mouse line thus established transmitted the transgene at Mendelian frequency. When crossed inter se, viable homozygotes were obtained, but they bred poorly. The *Fgf4*$^{GOF}$ transgene was maintained on a mixed genetic background.

#### Genotyping and phenotypic analysis

The genotypes of embryos and adult mice were determined by PCR assays using DNA extracted from embryonic yolk sacs or tails as a template. The presence of the *Fgf4*$^{GOF}$ allele was detected using primers that amplify the *lacZ* sequence in the transgene (5′-GTCTCGTTGCTGCATAAACC-3′ and 5′-TCGTCTGCTCATCCATGACC-3′). Genotyping for *Fgf8* alleles and for the presence of the *Msx2-cre* transgene was performed as previously described (Sun et al., 2002).

Embryos were collected in cold PBS, fixed in 4% paraformaldehyde and stored in 70% methanol at –20°C. Noon of the day when a vaginal plug was detected was considered approximately embryonic day (E) 0.5. To stage embryos more precisely, the somites posterior to the forelimb bud were counted and the total number of somites was determined by scoring the first one counted as somite 13. Standard protocols were employed for RNA in situ hybridizations and skeletal preparations. Assays for cell death were performed in whole mount, by staining with LysoTracker (Molecular Probes L-7528) (Grieshammer et al., 2005).

#### Quantification of *Fgf4* RNA

Limb buds were dissected from 5 *Msx2*-cre;*Fgf4*$^{GOF}$ and two control (*Msx2-cre* hemizygous) embryos at E10.5 and preserved in RNAlater (Ambion, 7020). Each sample contained either the two forelimb buds or the two hindlimb buds from an individual embryo. Total RNA was isolated using an RNeasy Kit (Qiagen 74104). First-strand cDNA synthesis was performed by the Biomolecular Resource Center at UCSF using a Bio-Rad kit (170-8891). Quantitative PCR was performed using an ABI Prism 7900 HT Sequence Detection System. The primers amplified a 57 bp sequence spanning sequences at the 3′ end of exon 2 to sequences at the 5′ end of exon 3 of the *Fgf4* gene: forward primer 5′-GAAAGGCACACCGAAGAGCTT-3′ and reverse primer 5′-GCCAGCCGGTTCTTCGT-3′. The sequence of the *Fgf4* TaqMan probe was 5′-CCTGCTGCTCATAGC-3′. *Gapdh* sequences were also amplified and the amount of product was used to normalize each sample.

## RESULTS

### Cre-mediated activation of an *Fgf4* conditional gain-of-function allele in the limb bud

To determine the effect of increasing *Fgf4* expression in the limb bud, we produced a mouse line carrying the *Fgf4*$^{GOF}$ transgene illustrated in Fig. 1A (see Materials and methods). Assays for β-gal activity at various stages of development demonstrated that prior to Cre-mediated recombination, the CAGG promoter in this transgene, which contains CMV enhancer/chicken β-actin sequences (Niwa et al., 1991), drives expression of a floxed (flanked by *loxP* sites) β-*Geo* reporter gene in most or all cells of the embryo (Fig. 1B, and data not shown). After Cre-mediated recombination, which excises the intervening floxed β-*Geo* sequences, the promoter drives expression of an *Fgf4* cDNA (Fig. 1A) in the cells in which recombination occurred and their descendants, presumably for as long as they survive. *Fgf4*$^{GOF}$ mice were crossed to animals carrying *Msx2-cre,* a transgene that expresses *cre* in early limb bud ectoderm, as well as in other tissues of the embryo. We previously used *Msx2-cre* to inactivate *Fgf4* (Sun et al., 2000), *Fgf8* (Lewandoski et al., 2000), and both *Fgf4* and *Fgf8* (Sun et al., 2002) during limb development. At birth, *Msx2-cre*;*Fgf4*$^{GOF}$ offspring were present at Mendelian frequency and were viable, but generally grew more slowly than did their wild-type littermates. All *Msx2-cre*;*Fgf4*$^{GOF}$ animals displayed limb abnormalities, as described below, as well as hyperplasia of the eyelids, malformations of the external genitalia and other defects (not shown). These animals carrying the activated transgene (A-Tg) are described here in comparison with their 'normal' littermates, which were wild-type or carried either *Msx2-cre* or *Fgf4*$^{GOF}$, but not both transgenes.

During normal limb development, *Fgf4* is expressed only after the AER has fully formed, and therefore *Fgf4* RNA is not detected until the 29- to 30-somite stage (ss) (~E10.0) in forelimb (FL) and 33-34 ss (~E10.25) in hindlimb (HL) buds (Sun et al., 2000) (Fig. 1D,F,H,J). At these stages and later, *Fgf4* expression is normally restricted to the posterior two-thirds of the AER (Niswander and Martin, 1992) (Fig. 1H,L,M), and ceases by ~E11.5 in FL and ~E12.5 in HL buds (Lewandoski et al., 2000) (Fig. 1N-Q). By contrast, in *Msx2*-cre;*Fgf4*$^{GOF}$ embryos, as a result of *Msx2-cre* activity in the early limb bud (Sun et al., 2000), *Fgf4* RNA was already detected at 28 ss in FL and 30 ss in HL buds, in a domain that was abnormally extended anteriorly (Fig. 1E,G,I,K, and data not shown). At ~E10.5, *Fgf4* expression was detected throughout the entire AP length of the AER (Fig. 1L,M). Moreover, *Fgf4* expression persisted for at least 1 day longer than normal, until the AER itself regressed (Fig. 1N-S). Together, these data show that in *Msx2*-cre;*Fgf4*$^{GOF}$ limb buds, *Fgf4* expression is initiated earlier, extends throughout a longer domain and persists for longer than in normal limb buds. In these respects, the expression of *Fgf4* in *Msx2*-cre;*Fgf4*$^{GOF}$ limb buds was more similar to that of *Fgf8* than *Fgf4* in normal limb buds.

We detected one significant difference between *Fgf4* expression in *Msx2*-cre;*Fgf4*$^{GOF}$ limb buds and the normal expression patterns of both *Fgf4* and *Fgf8*. In the normal embryo, *Fgf4* RNA is never detected in ventral limb bud ectoderm, and *Fgf8* RNA is detected in that domain only transiently, presumably in AER progenitors before they move distally and become incorporated into the nascent AER (Guo et al., 2003). By contrast, because *Msx2-cre* is active in a few cells that remain in the ventral ectoderm (Barrow et al., 2003), *Fgf4* RNA was detected at a low level in the ventral ectoderm of *Msx2*-cre;*Fgf4*$^{GOF}$ limb buds from early stages until at least E10.5 and presumably longer (Fig. 1I; data not shown).

To quantify the increase in *Fgf4* expression in *Msx2*-cre;*Fgf4*$^{GOF}$ limb buds at E10.5, we performed a quantitative RT-PCR assay (see Materials and methods). The level of *Fgf4* RNA was found to be 3.5-fold higher in FL and twofold higher in HL buds from *Msx2*-cre;*Fgf4*$^{GOF}$ embryos than from control (*Msx2-cre* hemizygous) embryos (Fig. 1C). From our in situ hybridization data, it is clear that at this stage, some of the *Fgf4* expressed by the activated *Msx2-cre*;*Fgf4*$^{GOF}$ transgene is localized in two ectopic domains, i.e. regions in which *Fgf4* is never expressed in the normal limb bud: one in the anterior AER, where *Fgf8* is normally expressed, and the other

in the ventral ectoderm, where AER-FGF gene expression is not normally detected. Because *Msx2-cre* is known to function throughout the AER (Sun et al., 2000), the remainder of the *Fgf4* produced by the activated *Fgf4*$^{GOF}$ transgene is presumably localized within the normal *Fgf4* expression domain in the posterior AER. However, expression of *Fgf4* in this domain occurs both earlier and for longer than normal in *Msx2-cre*;*Fgf4*$^{GOF}$ limb buds.

## Effects of activating *Fgf4*$^{GOF}$ on the AER-FGF/Sonic Hedgehog positive feedback loop

Before assessing the effects of the excess/ectopic *Fgf4* expression on limb morphogenesis, we examined *Msx2-cre*;*Fgf4*$^{GOF}$ limb buds to determine whether the AER itself or the expression of other AER-FGF genes was perturbed. *Fgf8* expression appeared normal in *Msx2-cre*;*Fgf4*$^{GOF}$ limb buds at E10.5 and E11.5 (Fig. 2A-B′, and data not shown), indicating that the AER, both with respect to its length along the AP axis and its width along the dorsoventral (D-V) axis, was normal. The expression of the other AER-FGF genes, *Fgf9* and *Fgf17*, also appeared similar in *Msx2-cre*;*Fgf4*$^{GOF}$ and normal limb buds (data not shown). Significantly, we found that at E13.5, *Fgf8* expression was detected in both normal and *Msx2-cre*;*Fgf4*$^{GOF}$ limb buds in a thin domain at the distal tip of each of the developing digits, but not in the regions overlying the interdigital mesenchyme (Fig. 2C,D, and data not shown). These observations indicate that the AER regresses at the same stage in *Msx2*-cre;*Fgf4*$^{GOF}$ and normal limb buds. One consistent difference we observed was that by E11.5 the limb buds of the *Msx2-cre*;*Fgf4*$^{GOF}$ embryos were slightly larger than those of their normal littermates (Fig. 1N-Q).

As signaling by AER-FGFs is thought to influence outgrowth and patterning of the limb bud mesenchyme, at least in part via its contribution to a positive feedback loop involving Sonic hedgehog (*Shh*) and its downstream target Gremlin (*Grem1*) (Laufer et al., 1994; Niswander et al., 1994; Zuniga et al., 1999; Khokha et al., 2003; Michos et al., 2004; Scherz et al., 2004), we next investigated whether *Shh* or *Grem1* expression was affected in *Msx2-cre*;*Fgf4*$^{GOF}$ limb buds. We found that both *Shh* and *Grem1* expression patterns appeared normal at ~E10.5 (Fig. 2E-H). However, at ~E11.5 we detected a significant abnormal expansion of the *Shh* expression domain both ventrally and especially proximally, with the effect being much more pronounced in HL than in FL buds (Fig. 2I,J). *Grem1* expression was similarly affected, but to a lesser extent (Fig. 2K,L). Analysis of sections through the limb buds demonstrated that these ectopic *Shh* and *Grem1* expression domains were localized exclusively in the mesenchyme (data not shown). Such ectopic mesenchyme gene expression in the *Msx2-cre*;*Fgf4*$^{GOF}$ limb buds might be due to either excess FGF4 produced in the AER, or more likely to ectopic *Fgf4* expression in the ventral ectoderm (Fig. 1I; data not shown), because the expansion of the *Shh* and *Grem1* expression domains was detected in ventral but not dorsal limb bud mesenchyme, and was not observed in the distal-most region near the AER.

## Activation of *Fgf4*$^{GOF}$ results in postaxial polydactyly and other autopod skeletal abnormalities

We next determined the consequences for skeletal patterning of the excess/ectopic *Fgf4* expression in *Msx2-cre*;*Fgf4*$^{GOF}$ limb buds. Analysis of eight *Msx2-cre*;*Fgf4*$^{GOF}$ postnatal skeletons revealed that the stylopod and zeugopod were normal, but the autopod was not (Fig. 3A-F; data not shown). In all 32 limbs examined, there was a supernumerary digit on the posterior side, containing a partial or, more frequently, a complete metacarpal/metatarsal and one or two phalanges (Fig. 3B,E). The metacarpal/metatarsal was generally fused to the posterior side of the metacarpal/metatarsal of digit V. In a few cases, there were additional phalanx-like elements between digit V and the supernumerary digit (Fig. 3C). In addition, in eight out of 16 hindlimbs, but in none of the forelimbs, there was a very

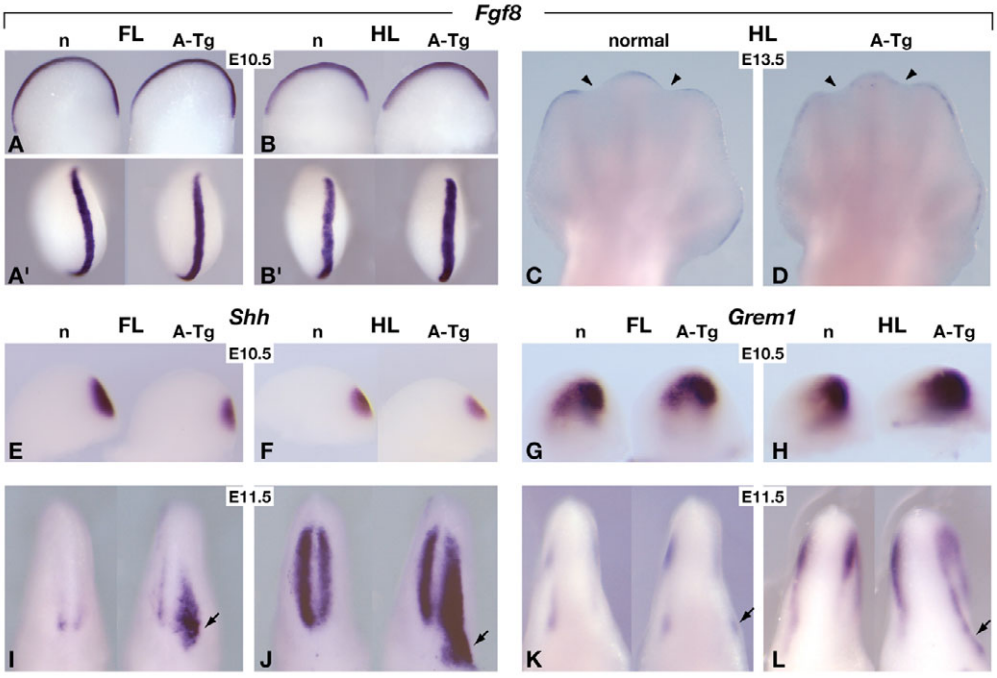


**Fig. 2. *Fgf8, Shh* and *Grem1* expression in *Msx2-cre*;*Fgf4*$^{GOF}$ limb buds.** (**A**-**L**) Whole-mount RNA in situ hybridization assays for the genes indicated in normal (n) and *Msx2-cre*;*Fgf4*$^{GOF}$ (A-Tg) limb buds. (A,B) Individual limb buds at E10.5 are shown in dorsal (anterior towards the left) view. In A′ and B′, the same limb buds are shown in distal view (dorsal towards the left). The AER, as marked by *Fgf8* expression, is of similar AP length and DV width in the normal and *Msx2-cre*;*Fgf4*$^{GOF}$ limb buds. (C,D) Hindlimbs at E13.5 are shown in dorsal view (anterior towards the left). In both normal and *Msx2-cre*;*Fgf4*$^{GOF}$ limb buds, the AER, as marked by *Fgf8* expression, is still present in regions covering the developing digits, but is no longer present over the regions covering the interdigital mesenchyme (arrowheads). This shows that AER regression is not delayed in *Msx2-cre*;*Fgf4*$^{GOF}$ limb buds. (E-H) Dorsal views at E10.5, with anterior towards the left. (I-L) Posterior views at E11.5, with dorsal leftwards, distal towards the top. Arrows indicate the regions in which the *Shh* and *Grem1* expression domains are expanded on the ventral side of the *Msx2-cre*;*Fgf4*$^{GOF}$ limb buds.

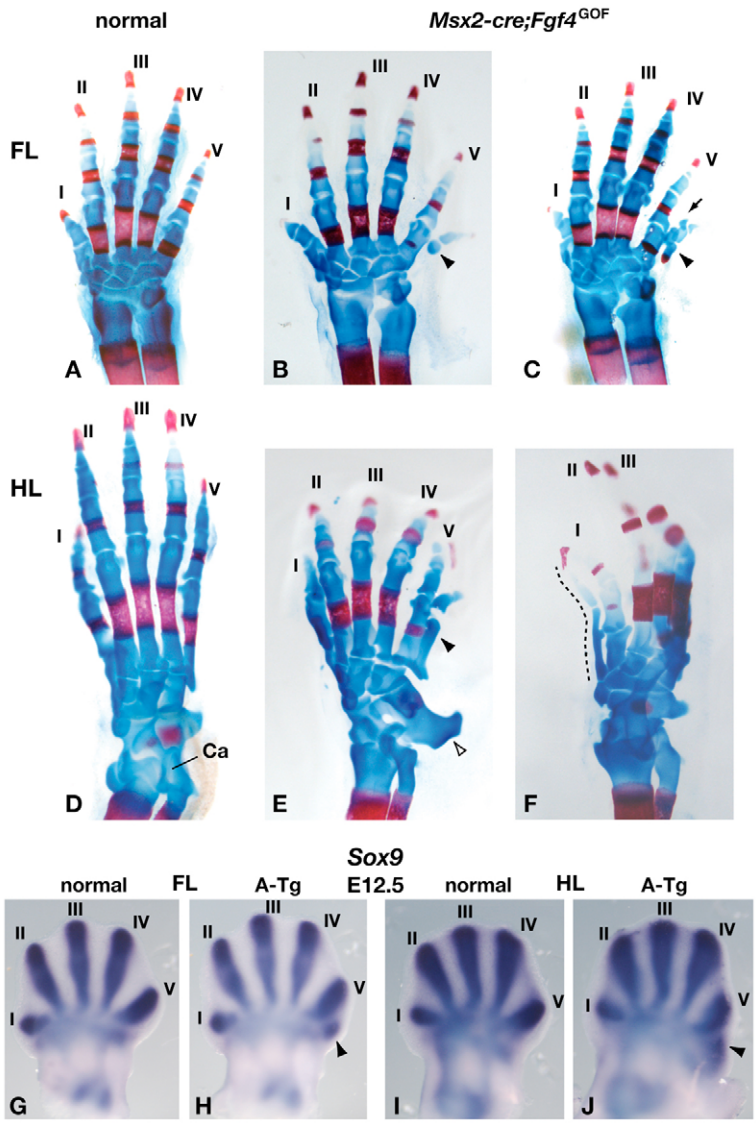


**Fig. 3. Limb skeletal abnormalities in *Msx2-cre;Fgf4*$^{GOF}$ mice.** (**A**-**F**) Skeletal preparations of newborn mouse limbs, with cartilage stained blue and bone stained red. Individual digits are numbered I-V, from anterior to posterior. (A-E) Dorsal views of autopods from normal and *Msx2-cre;Fgf4*$^{GOF}$ mice. The supernumerary posterior digit present in all animals that expressed the *Msx2-cre*-activated *Fgf4*$^{GOF}$ transgene is indicated by a filled arrowhead. The arrow in C indicates additional supernumerary phalanges found in some of these animals. The calcaneus (Ca) is enlarged in the *Msx2-cre;Fgf4*$^{GOF}$ hindlimb (open arrowhead in E). (F) Anterior view of an *Msx2-cre;Fgf4*$^{GOF}$ hindlimb containing a thin digit-like structure ventral to digit I (broken line). (**G**-**J**) Whole-mount in situ hybridization for *Sox9* expression in normal and *Msx2-cre;Fgf4*$^{GOF}$ (A-Tg) limb buds at E12.5. The condensations that prefigure the supernumerary posterior digit are evident at this stage (arrowheads in H and J).

thin digit-like structure ventral to digit I, which was detected when the limbs were viewed from the anterior side. It consisted of a partial or more complete metatarsal, and one or two phalanges, the most distal of which was sometimes attached to the distal phalanx of digit I (Fig. 3F; data not shown). We also found that in all *Msx2-cre;Fgf4*$^{GOF}$ hindlimbs, the proximal calcaneus was significantly enlarged (Fig. 3E). This largest of the eight elements that comprise the tarsus (ankle) is the most proximal tarsal element on the posterior side. Other carpal and tarsal elements appeared normal, although occasionally fusions of two elements were observed. Together, these data show that the effects on skeletal development of expressing *Fgf4* throughout the AER as well as in the ventral ectoderm are most pronounced on the posterior side of the limb.

An in situ hybridization assay for *Sox9*, the earliest known marker of skeletal element progenitors (Wright et al., 1995; Akiyama et al., 2002), showed that as early as E12.5, a supernumerary skeletal condensation was present posterior to the condensation representing digit V (Fig. 3G-J). At this stage, there were no obvious supernumerary condensations on the anterior ventral side of *Msx2-cre;Fgf4*$^{GOF}$ limb buds. These data indicate that formation of the supernumerary postaxial digit occurred during limb bud stages (prior to the regression of the AER).

## Activation of *Fgf4*$^{GOF}$ results in persistence of interdigital tissue

Another abnormality observed in *Msx2-cre;Fgf4*$^{GOF}$ autopods was the presence of soft tissue between the digits (Fig. 4A-D), a phenotype presumably caused by a lack of the interdigital programmed cell death (IPCD) that normally occurs in the mouse limb at ~E12.5-13.5. To confirm this, we assayed *Msx2-cre;Fgf4*$^{GOF}$ embryos at ~E13.5 by staining with LysoTracker, which labels acidic compartments (lysosomes) within apoptotic cells themselves as well as in healthy cells that are engulfing apoptotic debris (Zucker et al., 1999; Schaefer et al., 2004). In hindlimbs of normal embryos, intense LysoTracker staining was observed in the interdigital mesenchyme (Fig. 4E,E′); by contrast, we saw little or no LysoTracker staining in the hindlimbs of their *Msx2-cre;Fgf4*$^{GOF}$ littermates (Fig. 4F,F′). These data suggest that abnormally prolonged expression of *Fgf4* in the AER (see Fig. 1N-Q), or possibly a low level of ectopic expression in the ventral ectoderm, prevents cell death in the interdigital mesenchyme of *Msx2-cre;Fgf4*$^{GOF}$ embryos.

There is an extensive literature indicating that IPCD in the chicken embryo is mediated by BMP signaling and showing that IPCD can be prevented by ectopic expression of BMP antagonists (Zuzarte-Luis and Hurle, 2005). To determine whether the observed lack of

IPCD in *Msx2-cre*;*Fgf4*$^{GOF}$ limb buds was correlated with changes in the level of expression of genes involved in BMP signaling, we assayed for *Bmp2* and *Bmp7*, two members of the BMP family known to be expressed in the interdigital mesenchyme (Hogan, 1996), for *Msx2*, which is thought to be a downstream target of BMP signaling in the limb (Pizette et al., 2001), and for *Grem1*, which encodes an antagonist of BMP signaling in the limb (Hsu et al., 1998; Khokha et al., 2003; Michos et al., 2004). In situ hybridization assays showed no reproducible difference in the expression of these genes in *Msx2-cre*;*Fgf4*$^{GOF}$ when compared with normal limb buds at E12.5 (Fig. 4G-J), approximately 1 day earlier than the stage at which IPCD was detected in normal but not in *Msx2-cre*;*Fgf4*$^{GOF}$ hindlimb buds. These data suggest that excess/ectopic *Fgf4* expression prevents IPCD via a mechanism that does not involve changes in the expression of genes involved in BMP signaling.

### Activation of *Fgf4*$^{GOF}$ rescues the skeletal defects caused by loss of *Fgf8* function

Finally, we sought to determine whether the *Fgf4* expressed by the activated *Fgf4*$^{GOF}$ transgene can functionally replace *Fgf8* expression in the limb bud. We crossed male mice carrying both *Msx2-cre* and an *Fgf8* null allele, *Fgf8*$^{\Delta}$, to females carrying an *Fgf8* conditional allele, *Fgf8*$^{flox}$, and *Fgf4*$^{GOF}$, to generate *Msx2-cre*;*Fgf8*$^{\Delta/flox}$;*Fgf4*$^{GOF}$ mice. In these animals, *Msx2-cre*-mediated recombination inactivates *Fgf8* by converting *Fgf8*$^{flox}$ to a null allele and concomitantly activates *Fgf4* expression from the *Fgf4*$^{GOF}$ transgene. *Msx2-cre*;*Fgf8*$^{\Delta/flox}$ littermates from this cross displayed an *Fgf8* loss-of-function phenotype similar to, but somewhat less severe than that previously described (Lewandoski et al., 2000): the FL stylopod was usually mildly hypoplastic and missing the deltoid tuberosity (Fig. 5A,E), whereas the HL stylopod was often severely reduced (Fig. 5B,F); the zeugopod elements were mildly hypoplastic (Fig. 5A,B,E,F); and the autopod was frequently missing a digit: digit II or III in the forelimb (Fig. 5C,G, and data not shown) and digit I in the hindlimb (Fig. 5D,H). In addition, FL digits I and V and HL digits II and V were frequently missing a phalanx (Fig. 5C,D,G,H; data not shown).

Significantly, the defects that result from loss of *Fgf8* function were completely rescued in all *Msx2-cre*;*Fgf8*$^{\Delta/flox}$;*Fgf4*$^{GOF}$ skeletons. Thus, the deltoid tuberosity was always present (Fig. 5I), the femur appeared normal (Fig. 5J), and digits I-V were all present in both the FL and HL autopod and contained the normal number of phalanges (Fig. 5K,L). However, all *Msx2-cre*;*Fgf8*$^{\Delta/flox}$;*Fgf4*$^{GOF}$ limbs examined ($n$=7) still displayed the abnormalities observed when the *Fgf4*$^{GOF}$ transgene was activated by *Msx2-cre* in embryos that were wild type for *Fgf8* (Fig. 3), including enlargement of the calcaneus and a supernumerary posterior digit (Fig. 5I-L), as well as cutaneous syndactyly (data not shown). It is not clear precisely which aspects of the *Msx2-cre*-activated *Fgf4*$^{GOF}$ expression pattern are responsible for each of these specific abnormalities (see Discussion). What is most important about these data is that they clearly demonstrate that *Fgf4* is capable of performing the functions of *Fgf8* that are essential for normal limb skeletal development.

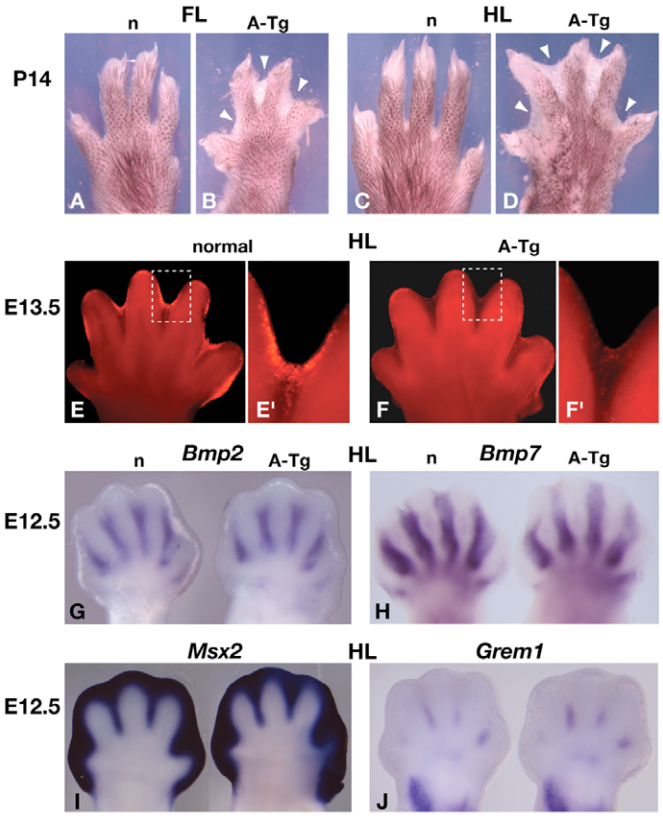


**Fig. 4. Persistence of interdigital tissue in *Msx2-cre*;*Fgf4*$^{GOF}$ limbs and effects on the expression of genes involved in BMP signaling.** (**A**-**D**) Limbs of normal (n) and *Msx2-cre*;*Fgf4*$^{GOF}$ (A-Tg) mice on postnatal day (P) 14, with the digits spread to illustrate the cutaneous syndactyly (white arrowheads). The supernumerary posterior digit is not visible in intact limbs. (**E**,**F**) Hindlimbs at E13.5 stained with Lysotracker to label regions with dying cells. The boxes in E and F indicate the regions shown at higher magnification in E′ and F′, respectively. (**G**-**J**) Hindlimb buds of normal and *Msx2-cre*;*Fgf4*$^{GOF}$ (A-Tg) mice at E12.5, hybridized in whole mount with probes for the genes indicated.

## DISCUSSION

The importance of FGF signaling from the AER to the limb bud mesenchyme is firmly established, but the functional significance of the expression of multiple FGF family members in the AER is not well understood. Using a Cre-mediated conditional gain-of-function strategy, we have shown that the excess/ectopic expression of *Fgf4* that results from activation of an *Fgf4*$^{GOF}$ transgene by *Msx2-cre* function causes postaxial polydactyly and other skeletal abnormalities, as well as cutaneous syndactyly between all the digits. These data underscore the importance for normal limb morphogenesis of precisely controlling the amount and spatiotemporal aspects of AER-FGF gene expression. Furthermore, using a novel approach for assessing the functional equivalence of genes in the mouse, we have demonstrated that FGF4 can perform the function(s) of FGF8 in patterning the limb skeleton.

### AER-FGF function in skeletal patterning

Based on the results of AER-FGF gene inactivation studies, it has been proposed that a key role of AER-FGF signaling is to establish the number of chondrocyte progenitors available to form limb skeletal elements (Sun et al., 2002), as a result of an anti-apoptotic effect and/or stimulation of cell proliferation. Our data, showing that the excess/ectopic *Fgf4* expression in *Msx2-cre*;*Fgf4*$^{GOF}$ limb buds results in the formation of supernumerary skeletal elements, are consistent with this hypothesis. However, because the normal pattern of *Fgf4* expression is altered in several ways in *Msx2-cre*;*Fgf4*$^{GOF}$ limb buds (including increased and prolonged expression in the posterior AER, and ectopic expression in the anterior AER and

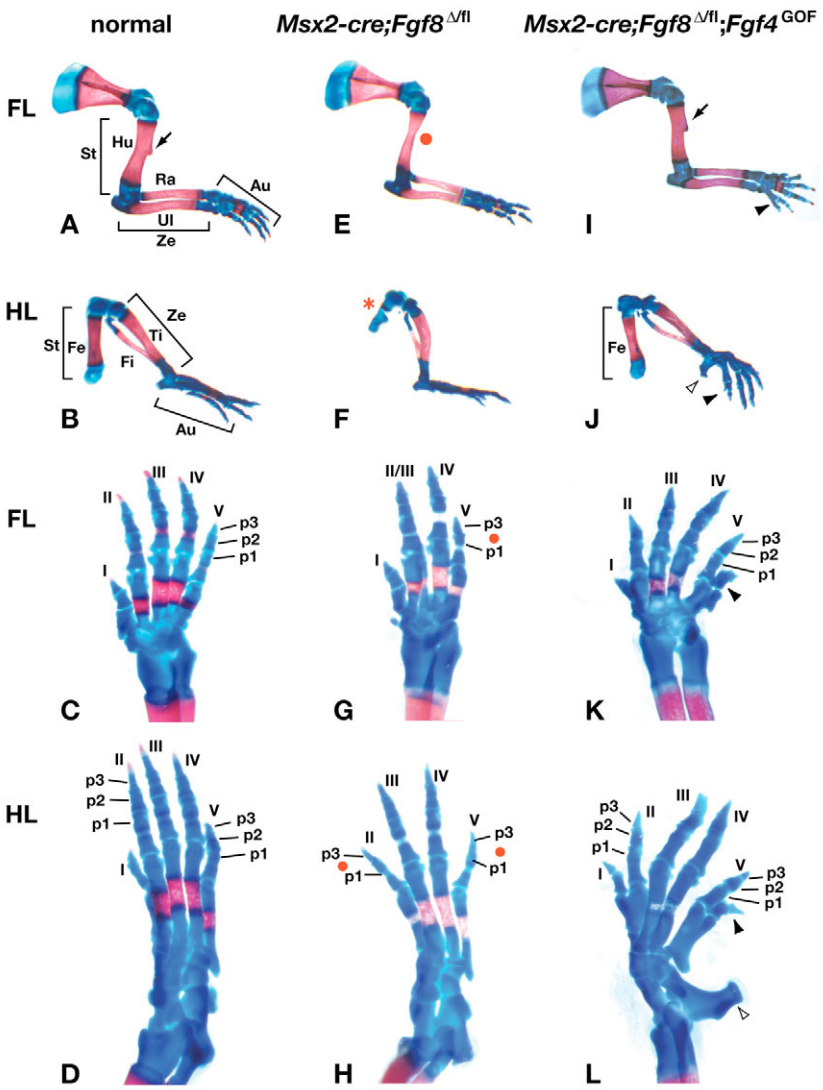


**Fig. 5. Rescue of the skeletal defects in *Msx2-cre;Fgf8*$^{\Delta/fl}$ mice by expression of the *Msx2-cre*-activated *Fgf4*$^{GOF}$ transgene.** (**A**-**L**) Skeletal preparations of newborn mouse limbs, with cartilage stained blue and bone stained red. In *Msx2-cre;Fgf8*$^{\Delta/flox}$ mice, the deltoid tuberosity, a feature of the normal humerus (arrows in A and I), is absent (red circle in E), the femur is extremely hypoplastic (red asterisk in F), one digit is missing and phalanges are absent from some of the remaining digits (red circles in G,H). All of these defects are rescued in *Msx2-cre;Fgf8*$^{\Delta/flox}$*;Fgf4*$^{GOF}$ limbs (I-L). Solid and open arrowheads indicate the posterior supernumerary digit and enlarged calcaneus, respectively, in *Msx2-cre;Fgf8*$^{\Delta/flox}$*;Fgf4*$^{GOF}$ limbs. Individual digits are numbered I-V, from anterior to posterior; phalanges (p) are numbered 1-3, from proximal to distal. Abbreviations: Au, autopod; Fe, femur; Fi, fibula; Hu, humerus; Ra, radius; St, stylopod; Ti, tibia; Ul, ulna; Ze, zeugopod.

ventral ectoderm), we can only speculate on the source of the FGF4 that causes the observed defects in the autopod skeleton.

For example, the ventral location of the thin anterior digit-like structure found in many *Msx2-cre*;*Fgf4*$^{GOF}$ hindlimbs suggests that it forms in response to ectopic *Fgf4* expression in either the ventral ectoderm or the anterior AER. By contrast, it seems likely that excess *Fgf4* expression in the posterior AER is responsible for the formation a supernumerary digit on the posterior side of *Msx2-cre*;*Fgf4*$^{GOF}$ limbs, based on evidence from several mouse mutants. For example, mice with mutations in *Dkk1* (Adamska et al., 2003; MacDonald et al., 2004) or in which the BMP antagonist Noggin is ectopically expressed in the AER (Wang et al., 2004) display an increase in AER-FGF expression and have a supernumerary digit on the posterior side. However, if the supernumerary posterior digit in *Msx2-cre*;*Fgf4*$^{GOF}$ limbs is indeed due to excess FGF expression in the AER, then why does an extra digit still form in *Msx2-cre*;Fgf8$^{\Delta/flox}$;*Fgf4*$^{GOF}$ limbs, which lack *Fgf8* expression? A possible explanation comes from the observation that in the absence of *Fgf8* function in the AER, endogenous *Fgf4* expression is significantly upregulated (Lewandoski et al., 2000; Moon and Capecchi, 2000), although obviously not to the level needed for formation of the normal complement of skeletal elements. Thus, we suggest that the AER-FGF produced by the expression of the activated *Fgf4*$^{GOF}$ transgene in combination with the normal levels of endogenous *Fgf4* and *Fgf8* expression in *Msx2-cre;Fgf4*$^{GOF}$ limbs or in combination with upregulated endogenous *Fgf4* expression in *Msx2-cre*;*Fgf8*$^{\Delta/flox}$;*Fgf4*$^{GOF}$ limb buds, is sufficient to produce six digits.

We were surprised to find that *Msx2-cre*;*Fgf4*$^{GOF}$ limbs did not contain one or more supernumerary digits on the anterior side of the limb, because there are numerous mouse mutants in which *Fgf4* expression in the anterior AER is correlated with such preaxial polydactyly (Masuya et al., 1995; Qu et al., 1997; Hayes et al., 1998; Yang et al., 1998; Yada et al., 2002; Zhang et al., 2003). However, in those mutants the anterior expansion of the *Fgf4* expression domain appears to be a secondary response to ectopic Hedgehog pathway activity in the anterior mesenchyme (Talamillo et al., 2005; Liu et al., 2005). As yet, there are no data addressing the issue of whether such ectopic *Fgf4* expression in the anterior AER is necessary for the formation of the supernumerary preaxial digit(s).

Together, the data suggest a model in which excess AER-FGF signaling per se promotes the formation of a supernumerary digit on the posterior side, possibly by increasing SHH signaling or by expanding the number of descendants of *Shh*-expressing cells, which are known to contribute to posterior digits (Ahn and Joyner, 2004; Harfe et al., 2004). By contrast, changes in the expression of other

genes, such as those that cause ectopic Hedgehog pathway activity in anterior mesenchyme, are required for supernumerary digit formation on the anterior side. According to this model, the postaxial and preaxial polydactyly reported in mouse hindlimbs in which *Bmp4* has been conditionally inactivated in the mesenchyme (Selever et al., 2004) can be explained by two separate effects: the supernumerary posterior digit forms in response to an observed increase in AER-FGF gene expression resulting from expansion of the AER along the DV axis, and the additional supernumerary anterior digit forms as a consequence of other changes in gene expression in the anterior mesenchyme. In this context it is interesting that in embryos null for both *Msx1* and *Msx2*, which are thought to be required for BMP signaling, preaxial polydactyly seems to correlate with a very small ectopic anterior domain of *Shh* expression (Lallemand et al., 2005). However, it is important to note that anterior mesenchyme is capable of forming supernumerary digits in response to FGF signaling, as for example in transgenic mice expressing a hypermorphic allele of *Fgfr1* (Hajihosseini et al., 2004), and in chicken limb buds implanted with cells producing FGF2 (Riley et al., 1993). Curiously, in the latter experiments, posterior mesenchyme showed no response to FGF2-producing grafts. Further studies will be needed to elucidate the mechanism(s) that regulate digit number and determine the location(s) at which supernumerary digits form.

## AER-FGF function in regulating interdigital programmed cell death

In addition to abnormalities in skeletal pattern, *Msx2-cre*;*Fgf4*$^{GOF}$ limbs have cutaneous syndactyly between all the digits. As in many mouse mutants, such syndactyly correlates with a lack of interdigital programmed cell death (IPCD) (Zuzarte-Luis and Hurle, 2005). A potential link between AER-FGF signaling and IPCD is suggested by the hypothesis that AER-FGFs provide proliferation/survival factors for interdigital mesenchyme cells (Macias et al., 1996), and that under normal circumstances IPCD is triggered by the loss of these factors when the AER regresses. Thus, a delay in AER regression should delay or block IPCD and result in persistence of interdigital tissue. Support for this model comes from gain-of-function experiments in both chicken limb buds and transgenic mice, showing that ectopic expression of the BMP antagonist Noggin results in a delay in AER regression and cutaneous syndactyly (Pizette and Niswander, 1999; Wang et al., 2004). Based on those studies, it was proposed that during normal limb development, one role of BMP signaling is to promote AER regression. In support of this hypothesis, mice that lack both *Msx1* and *Msx2* function (Lallemand et al., 2005), or in which *Bmpr1a* has been inactivated in the AER (M. Lewandoski, personal communication), display abnormal AER regression and persistence of interdigital tissue.

However, AER regression does not appear to be delayed in *Msx2-cre*;*Fgf4*$^{GOF}$ limb buds, and other effects besides delay of AER regression are observed in mouse limb buds lacking *Msx1/Msx2* function, lacking *Bmpr1a* function in the AER, or with ectopic Noggin expression in the AER. In particular, the AER is expanded along its DV axis (Wang et al., 2004; Lallemand et al., 2005) (M. Lewandoski, personal communication), raising the possibility that excess/ectopic AER-FGF expression from the expanded AER, rather than a delay in AER regression per se, accounts for the observed persistence of interdigital tissue in those limb buds. If so, then the cutaneous syndactyly we observed in *Msx2-cre*;*Fgf4*$^{GOF}$ limbs might likewise be explained by excess/ectopic *Fgf4* expression in the AER, or perhaps in the ventral ectoderm. Such FGF signaling might directly oppose the pro-apoptotic effects of BMP signaling (Yokouchi et al., 1996; Zou and Niswander, 1996; Macias et al., 1997), as suggested by studies showing that implanting BMP4-soaked beads into interdigital mesenchyme causes cell death and this is prevented by co-implanting FGF2-soaked beads (Ganan et al., 1996). A more complex relationship between FGF and BMP signaling in the control of IPCD has also been suggested (Montero et al., 2001). Alternatively, excess FGF signaling might inhibit BMP activity via effects on genes involved in BMP signaling. However, we saw no effect on the expression of *Bmp2*, *Bmp4*, *Msx2* or *Grem1* in *Msx2-cre*;*Fgf4*$^{GOF}$ limb buds just prior to the stage when IPCD normally occurs. Further studies will be needed to unravel the potentially complex interactions between FGF and BMP signaling in the regulation of IPCD.

## FGF4 can replace FGF8 during vertebrate limb development

Although FGF4 and FGF8 belong to different subgroups of the FGF family (Itoh and Ornitz, 2004) and share only ~32% identity in the most conserved core domain (Coulier et al., 1997), they have been found to have similar activities in various developmental settings. For example, in the chicken embryo, beads soaked in recombinant FGF4 or FGF8 can induce the formation of an ectopic limb (Martin, 1998) and induce cells in the diencephalon to change fate and develop into a midbrain (Crossley et al., 1996). However, during gastrulation in the chicken embryo, primitive streak cells are attracted to a source of FGF4 and repelled by a source of FGF8 (Yang et al., 2002), indicating that these two FGF family members do not necessarily perform the same function in all developmental contexts. Genetic analyses in the mouse have left open the issue of whether FGF4 and FGF8 have similar or different functions in limb development.

To resolve this issue, we employed a novel approach to assess whether one gene can functionally replace another in the mouse, rather than the conventional knock-in strategy (Hanks et al., 1995), in which the sequence of one gene is inserted into the genomic locus of a second, thereby inactivating the second gene and expressing the first in its place. Instead, we replaced the expression of one gene (*Fgf8*) with that of another (*Fgf4*) by using a single *cre* transgene to concomitantly inactivate and activate conditional *Fgf8* loss- and *Fgf4* gain-of-function alleles, respectively, in the same cells. The knock-in strategy has the advantage that the gene that has been inserted should faithfully recapitulate the expression of the gene it is meant to replace, although this is sometimes difficult to achieve if regulatory elements that control the expression of the gene being replaced are perturbed. Using our strategy, the expression of the gain-of-function target gene may ultimately be broader than the gene expression it replaces, because it continues in all descendants of the cells in which it was initially activated. That was indeed the case in our study, as *Fgf4* expression, which is driven by the promoter in the transgene, persisted in the limb bud ventral ectoderm, whereas *Fgf8* expression, although initially detected in that domain, normally becomes restricted to the AER. As discussed above, such discrepancies between the expression patterns of the two genes can make interpretation of the data difficult. However, our strategy has some distinct advantages. First, an individual conditional gain-of-function transgene can be readily used in combination with various conditional loss-of-function alleles to study the functional relationships between different members of a multigene family. Second, the conditional gain-of-function transgene can be activated without inactivating any other gene, allowing analysis of the consequences of excess or ectopic expression of the gain-of-function target gene, in our case *Fgf4* in the limb bud. In future, *Fgf4*$^{GOF}$

could be activated in a variety of developmental settings using appropriate *cre* transgenes to gain further insights into the function of FGF signaling.

Here we made use of the $Fgf4^{GOF}$ transgene to show that all of the limb skeletal defects caused by loss of *Fgf8* function can be rescued by increasing *Fgf4* expression in the limb bud in a pattern that largely resembles that of *Fgf8* in normal limb buds. This demonstrates the utility of our strategy, and more importantly, provides conclusive evidence that FGF4 can functionally replace FGF8 in limb skeletal patterning. Furthermore, our data emphasize the importance of mechanisms that control FGF gene expression for obtaining normal digit number and appropriate separation of the digits.

We thank R. Harland, J. Hébert, N. Itoh, V. Lefebvre, D. Ornitz and J. Wozney for providing plasmids from which the probes for in situ hybridization were made. We also thank Deborah Kurrasch for expert advice on quantitative RT-PCR assays. We are grateful to Guijuan Qiao, Christina Ahn, Prajakta Ghatpande, Lisa Matsubara and Ariana Nemati for technical assistance, and to our colleagues in the Martin laboratory for critical comments on the manuscript. Contributors to this work were supported by: NIH training grant HL07731 (P.L.) and a KO8 award from the NIH (CA60538; G.M.). This work was supported by a grant RO1 HD34380 (to G.R.M.).

**References**

**Adamska, M., MacDonald, B. T. and Meisler, M. H.** (2003). Doubleridge, a mouse mutant with defective compaction of the apical ectodermal ridge and normal dorsal-ventral patterning of the limb. *Dev. Biol.* **255**, 350-362.

**Ahn, S. and Joyner, A. L.** (2004). Dynamic changes in the response of cells to positive hedgehog signaling during mouse limb patterning. *Cell* **118**, 505-516.

**Akiyama, H., Chaboissier, M. C., Martin, J. F., Schedl, A. and de Crombrugghe, B.** (2002). The transcription factor Sox9 has essential roles in successive steps of the chondrocyte differentiation pathway and is required for expression of Sox5 and Sox6. *Genes Dev.* **16**, 2813-2828.

**Barrow, J. R., Thomas, K. R., Boussadia-Zahui, O., Moore, R., Kemler, R., Capecchi, M. R. and McMahon, A. P.** (2003). Ectodermal Wnt3/beta-catenin signaling is required for the establishment and maintenance of the apical ectodermal ridge. *Genes Dev.* **17**, 394-409.

**Boulet, A. M., Moon, A. M., Arenkiel, B. R. and Capecchi, M. R.** (2004). The roles of Fgf4 and Fgf8 in limb bud initiation and outgrowth. *Dev. Biol.* **273**, 361-372.

**Capdevila, J. and Izpisua Belmonte, J. C.** (2001). Patterning mechanisms controlling vertebrate limb development. *Annu. Rev. Cell Dev. Biol.* **17**, 87-132.

**Colvin, J. S., Green, R. P., Schmahl, J., Capel, B. and Ornitz, D. M.** (2001). Male-to-female sex reversal in mice lacking fibroblast growth factor 9. *Cell* **104**, 875-889.

**Coulier, F., Pontarotti, P., Roubin, R., Hartung, H., Goldfarb, M. and Birnbaum, D.** (1997). Of worms and men: an evolutionary perspective on the fibroblast growth factor (FGF) and FGF receptor families. *J. Mol. Evol.* **44**, 43-56.

**Crossley, P. H. and Martin, G. R.** (1995). The mouse *Fgf8* gene encodes a family of polypeptides and is expressed in regions that direct outgrowth and patterning in the developing embryo. *Development* **121**, 439-451.

**Crossley, P. H., Martinez, S. and Martin, G. R.** (1996). Midbrain development induced by FGF8 in the chick embryo. *Nature* **380**, 66-68.

**Dudley, A. T., Ros, M. A. and Tabin, C. J.** (2002). A re-examination of proximodistal patterning during vertebrate limb development. *Nature* **418**, 539-544.

**Fallon, J., López, A., Ros, M., Savage, M., Olwin, B. and Simandl, B.** (1994). FGF-2: Apical ectodermal ridge growth signal for chick limb development. *Science* **264**, 104-107.

**Ganan, Y., Macias, D., Duterque-Coquillaud, M., Ros, M. A. and Hurle, J. M.** (1996). Role of TGF beta s and BMPs as signals controlling the position of the digits and the areas of interdigital cell death in the developing chick limb autopod. *Development* **122**, 2349-2357.

**Grieshammer, U., Cebrián, C., Ilagan, R., Meyers, E. N., Herzlinger, D. and Martin, G. R.** (2005). FGF8 is required for cell survival at distinct stages of nephrogenesis and for regulation of gene expression in nascent nephrons. *Development* **132**, 3847-3857

**Guo, Q., Loomis, C. and Joyner, A. L.** (2003). Fate map of mouse ventral limb ectoderm and the apical ectodermal ridge. *Dev. Biol.* **264**, 166-178.

**Hajihosseini, M. K., Lalioti, M. D., Arthaud, S., Burgar, H. R., Brown, J. M., Twigg, S. R., Wilkie, A. O. and Heath, J. K.** (2004). Skeletal development is regulated by fibroblast growth factor receptor 1 signalling dynamics. *Development* **131**, 325-335.

**Hanks, M., Wurst, W., Anson-Cartwright, L., Auerbach, A. B. and Joyner, A. L.** (1995). Rescue of the En-1 mutant phenotype by replacement of En-1 with En-2. *Science* **269**, 679-682.

**Harfe, B. D., Scherz, P. J., Nissim, S., Tian, H., McMahon, A. P. and Tabin, C. J.** (2004). Evidence for an expansion-based temporal Shh gradient in specifying vertebrate digit identities. *Cell* **118**, 517-528.

**Hayes, C., Brown, J. M., Lyon, M. F. and Morriss-Kay, G. M.** (1998). Sonic hedgehog is not required for polarising activity in the Doublefoot mutant mouse limb bud. *Development* **125**, 351-357.

**Hogan, B. L.** (1996). Bone morphogenetic proteins: multifunctional regulators of vertebrate development. *Genes Dev.* **10**, 1580-1594.

**Hooper, M., Hardy, K., Handyside, A., Hunter, S. and Monk, M.** (1987). HPRT-deficient (Lesch-Nyhan) mouse embryos derived from germline colonization by cultured cells. *Nature* **326**, 292-295.

**Hsu, D. R., Economides, A. N., Wang, X., Eimon, P. M. and Harland, R. M.** (1998). The Xenopus dorsalizing factor Gremlin identifies a novel family of secreted proteins that antagonize BMP activities. *Mol. Cell* **1**, 673-683.

**Itoh, N. and Ornitz, D. M.** (2004). Evolution of the Fgf and Fgfr gene families. *Trends Genet.* **20**, 563-569.

**Khokha, M. K., Hsu, D., Brunet, L. J., Dionne, M. S. and Harland, R. M.** (2003). Gremlin is the BMP antagonist required for maintenance of Shh and Fgf signals during limb patterning. *Nat. Genet.* **34**, 303-307.

**Lallemand, Y., Nicola, M. A., Ramos, C., Bach, A., Clement, C. S. and Robert, B.** (2005). Analysis of Msx1; Msx2 double mutants reveals multiple roles for Msx genes in limb development. *Development* **132**, 3003-3014.

**Laufer, E., Nelson, C. E., Johnson, R. L., Morgan, B. A. and Tabin, C.** (1994). Sonic hedgehog and Fgf-4 act through a signaling cascade and feedback loop to integrate growth and patterning of the developing limb bud. *Cell* **79**, 993-1003.

**Lewandoski, M., Sun, X. and Martin, G. R.** (2000). Fgf8 signalling from the AER is essential for normal limb development. *Nat. Genet.* **26**, 460-463.

**Liu, A., Wang, B. and Niswander, L. A.** (2005). Mouse intraflagellar transport proteins regulate both the activator and repressor functions of Gli transcription factors. *Development* **132**, 3103-3111.

**Lobe, C. G., Koop, K. E., Kreppner, W., Lomeli, H., Gertsenstein, M. and Nagy, A.** (1999). Z/AP, a double reporter for cre-mediated recombination. *Dev. Biol.* **208**, 281-292.

**MacDonald, B. T., Adamska, M. and Meisler, M. H.** (2004). Hypomorphic expression of Dkk1 in the doubleridge mouse: dose dependence and compensatory interactions with Lrp6. *Development* **131**, 2543-2552.

**Macias, D., Ganan, Y., Ros, M. A. and Hurle, J. M.** (1996). In vivo inhibition of programmed cell death by local administration of FGF-2 and FGF-4 in the interdigital areas of the embryonic chick leg bud. *Anat. Embryol. (Berl)* **193**, 533-541.

**Macias, D., Ganan, Y., Sampath, T. K., Piedra, M. E., Ros, M. A. and Hurle, J. M.** (1997). Role of BMP-2 and OP-1 (BMP-7) in programmed cell death and skeletogenesis during chick limb development. *Development* **124**, 1109-1117.

**Mahmood, R., Bresnick, J., Hornbruch, A., Mahony, C., Morton, N., Colquhoun, K., Martin, P., Lumsden, A., Dickson, C. and Mason, I.** (1995). A role for FGF-8 in the initiation and maintenance of vertebrate limb bud outgrowth. *Curr. Biol.* **5**, 797-806.

**Martin, G. R.** (1998). The roles of FGFs in the early development of vertebrate limbs. *Genes Dev.* **12**, 1571-1586.

**Martin, G. R. and Evans, M. J.** (1975). Differentiation of clonal lines of teratocarcinoma cells: formation of embryoid bodies in vitro. *Proc. Natl. Acad. Sci. USA* **72**, 1441-1445.

**Masuya, H., Sagai, T., Wakana, S., Moriwaki, K. and Shiroishi, T.** (1995). A duplicated zone of polarizing activity in polydactylous mouse mutants. *Genes Dev.* **9**, 1645-1653.

**Michos, O., Panman, L., Vintersten, K., Beier, K., Zeller, R. and Zuniga, A.** (2004). Gremlin-mediated BMP antagonism induces the epithelial-mesenchymal feedback signaling controlling metanephric kidney and limb organogenesis. *Development* **131**, 3401-3410.

**Montero, J. A., Ganan, Y., Macias, D., Rodriguez-Leon, J., Sanz-Ezquerro, J. J., Merino, R., Chimal-Monroy, J., Nieto, M. A. and Hurle, J. M.** (2001). Role of FGFs in the control of programmed cell death during limb development. *Development* **128**, 2075-2084.

**Moon, A. M. and Capecchi, M. R.** (2000). Fgf8 is required for outgrowth and patterning of the limbs. *Nat. Genet.* **26**, 455-459.

**Moon, A. M., Boulet, A. M. and Capecchi, M. R.** (2000). Normal limb development in conditional mutants of *Fgf4*. *Development* **127**, 989-996.

**Niswander, L. and Martin, G. R.** (1992). Fgf-4 expression during gastrulation, myogenesis, limb and tooth development in the mouse. *Development* **114**, 755-768.

**Niswander, L., Tickle, C., Vogel, A., Booth, I. and Martin, G. R.** (1993). FGF-4 replaces the apical ectodermal ridge and directs outgrowth and patterning of the limb. *Cell* **75**, 579-587.

**Niswander, L., Jeffrey, S., Martin, G. R. and Tickle, C.** (1994). A positive feedback loop coordinates growth and patterning in the vertebrate limb. *Nature* **371**, 609-612.

**Niwa, H., Yamamura, K. and Miyazaki, J.** (1991). Efficient selection for high-expression transfectants with a novel eukaryotic vector. *Gene* **108**, 193-199.

**Pizette, S. and Niswander, L.** (1999). BMPs negatively regulate structure and function of the limb apical ectodermal ridge. *Development* **126**, 883-894.
**Pizette, S., Abate-Shen, C. and Niswander, L.** (2001). BMP controls proximodistal outgrowth, via induction of the apical ectodermal ridge, and dorsoventral patterning in the vertebrate limb. *Development* **128**, 4463-4474.
**Qu, S., Niswender, K. D., Ji, Q., van der Meer, R., Keeney, D., Magnuson, M. A. and Wisdom, R.** (1997). Polydactyly and ectopic ZPA formation in Alx-4 mutant mice. *Development* **124**, 3999-4008.
**Riley, B. B., Savage, M. P., Simandl, B. K., Olwin, B. B. and Fallon, J. F.** (1993). Retroviral expression of FGF-2 (bFGF) affects patterning in chick limb bud. *Development* **118**, 95-104.
**Rowe, D. A. and Fallon, J. F.** (1982). The proximodistal determination of skeletal parts in the developing chick leg. *J. Embryol. Exp. Morphol.* **68**, 1-7.
**Rowe, D. A., Cairns, J. M. and Fallon, J. F.** (1982). Spatial and temporal patterns of cell death in limb bud mesoderm after apical ectodermal ridge removal. *Dev. Biol.* **93**, 83-91.
**Saunders, J. W., Jr** (1948). The proximo-distal sequence of the origin of the parts of the chick wing and the role of the ectoderm. *J. Exp. Zool.* **108**, 363-403.
**Schaefer, K. S., Doughman, Y. Q., Fisher, S. A. and Watanabe, M.** (2004). Dynamic patterns of apoptosis in the developing chicken heart. *Dev. Dyn.* **229**, 489-499.
**Scherz, P. J., Harfe, B. D., McMahon, A. P. and Tabin, C. J.** (2004). The limb bud Shh-Fgf feedback loop is terminated by expansion of former ZPA cells. *Science* **305**, 396-399.
**Selever, J., Liu, W., Lu, M. F., Behringer, R. R. and Martin, J. F.** (2004). Bmp4 in limb bud mesoderm regulates digit pattern by controlling AER development. *Dev. Biol.* **276**, 268-279.
**Summerbell, D.** (1974). A quantitative analysis of the effect of excision of the AER from the chick limb bud. *J. Embryol. Exp. Morphol.* **32**, 651-660.
**Sun, X., Lewandoski, M., Meyers, E. N., Liu, Y. H., Maxson, R. E., Jr and Martin, G. R.** (2000). Conditional inactivation of Fgf4 reveals complexity of signalling during limb bud development. *Nat. Genet.* **25**, 83-86.
**Sun, X., Mariani, F. V. and Martin, G. R.** (2002). Functions of FGF signalling from the apical ectodermal ridge in limb development. *Nature* **418**, 501-508.
**Talamillo, A., Bastida, M. F., Fernandez-Teran, M. and Ros, M. A.** (2005). The developing limb and the control of the number of digits. *Clin .Genet.* **67**, 143-153.
**Wang, C. K., Omi, M., Ferrari, D., Cheng, H. C., Lizarraga, G., Chin, H. J., Upholt, W. B., Dealy, C. N. and Kosher, R. A.** (2004). Function of BMPs in the apical ectoderm of the developing mouse limb. *Dev. Biol.* **269**, 109-122.
**Wright, E., Hargrave, M. R., Christiansen, J., Cooper, L., Kun, J., Evans, T., Gangadharan, U., Greenfield, A. and Koopman, P.** (1995). The Sry-related gene Sox9 is expressed during chondrogenesis in mouse embryos. *Nat. Genet.* **9**, 15-20.
**Xu, J., Liu, Z. and Ornitz, D. M.** (2000). Temporal and spatial gradients of *Fgf8* and *Fgf17* regulate proliferation and differentiation of midline cerebellar structures. *Development* **127**, 1833-1843.
**Yada, Y., Makino, S., Chigusa-Ishiwa, S. and Shiroishi, T.** (2002). The mouse polydactylous mutation, luxate (lx), causes anterior shift of the anteroposterior border in the developing hindlimb bud. *Int. J. Dev. Biol.* **46**, 975-982.
**Yang, X., Dormann, D., Munsterberg, A. E. and Weijer, C. J.** (2002). Cell movement patterns during gastrulation in the chick are controlled by positive and negative chemotaxis mediated by FGF4 and FGF8. *Dev. Cell* **3**, 425-437.
**Yang, Y., Guillot, P., Boyd, Y., Lyon, M. F. and McMahon, A. P.** (1998). Evidence that preaxial polydactyly in the Doublefoot mutant is due to ectopic Indian Hedgehog signaling. *Development* **125**, 3123-3132.
**Yokouchi, Y., Sakiyama, J., Kameda, T., Iba, H., Suzuki, A., Ueno, N. and Kuroiwa, A.** (1996). BMP-2/-4 mediate programmed cell death in chicken limb buds. *Development* **122**, 3725-3734.
**Zhang, Q., Murcia, N. S., Chittenden, L. R., Richards, W. G., Michaud, E. J., Woychik, R. P. and Yoder, B. K.** (2003). Loss of the Tg737 protein results in skeletal patterning defects. *Dev. Dyn.* **227**, 78-90.
**Zou, H. and Niswander, L.** (1996). Requirement for BMP signaling in interdigital apoptosis and scale formation. *Science* **272**, 738-741.
**Zucker, R. M., Hunter, E. S., 3rd and Rogers, J. M.** (1999). Apoptosis and morphology in mouse embryos by confocal laser scanning microscopy. *Methods* **18**, 473-480.
**Zuniga, A., Haramis, A. P., McMahon, A. P. and Zeller, R.** (1999). Signal relay by BMP antagonism controls the SHH/FGF4 feedback loop in vertebrate limb buds. *Nature* **401**, 598-602.
**Zuzarte-Luis, V. and Hurle, J. M.** (2005). Programmed cell death in the embryonic vertebrate limb. *Semin. Cell Dev. Biol.* **16**, 261-269.